

See discussions, stats, and author profiles for this publication at: <https://www.researchgate.net/publication/305718399>

First Evaluation on Single Photon-Sensitive Lidar Data

Article *in* Photogrammetric Engineering and Remote Sensing · July 2016

DOI: 10.14358/PERS.82.7.455

CITATIONS

2

READS

112

4 authors, including:



[John J. Degnan](#)

Sigma Space Corporation

222 PUBLICATIONS 2,801 CITATIONS

[SEE PROFILE](#)



[Jie Shan](#)

Purdue University

137 PUBLICATIONS 1,747 CITATIONS

[SEE PROFILE](#)

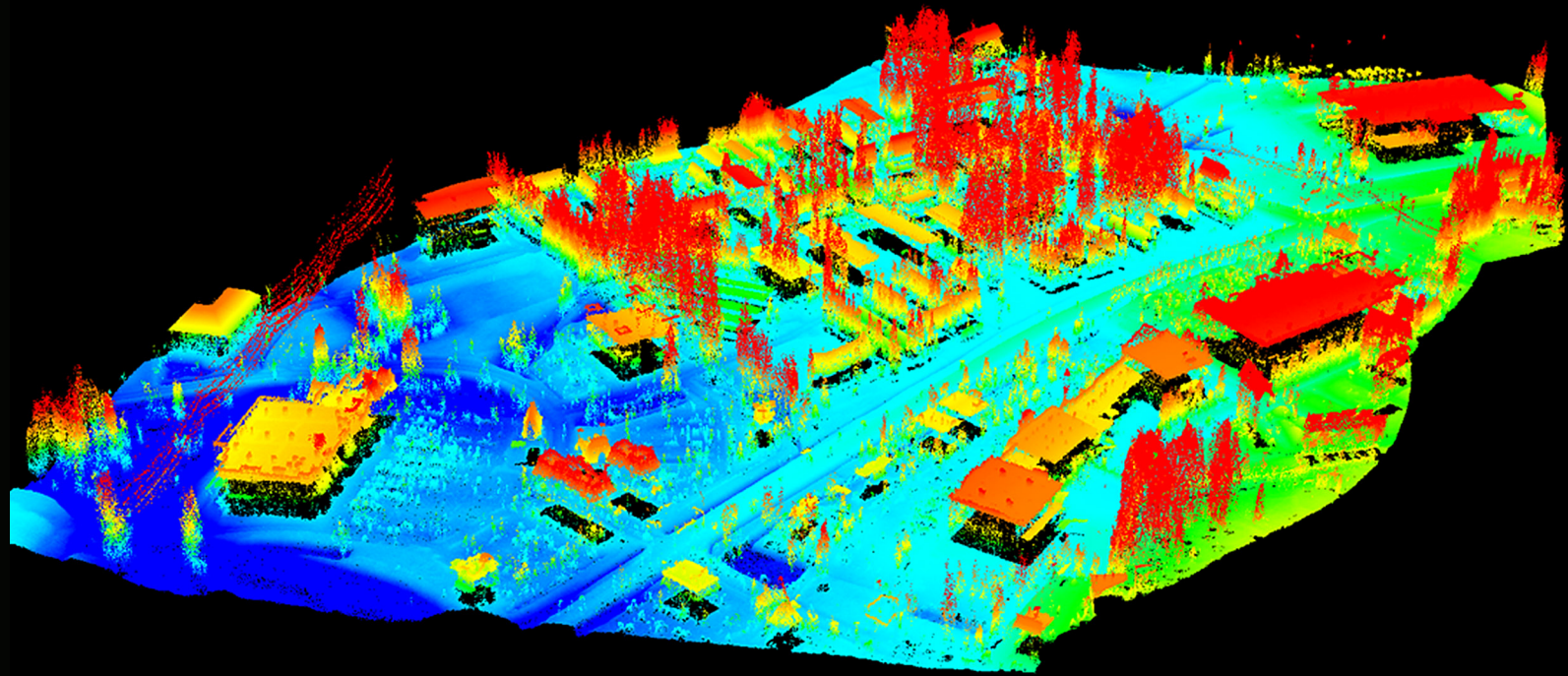
Some of the authors of this publication are also working on these related projects:



Single Photon Lidars for Large Scale 3D Topographic and Bathymetric Imaging [View project](#)



Space Geodesy Satellite Laser Ranging System (SGSLR) [View project](#)



First Evaluation on Single Photon-Sensitive Lidar Data

By Qinghua Li, John Degnan, Terence Barrett, and Jie Shan

Single Photon-sensitive Lidar or SPL (Degnan et al, 2015) was developed by Sigma Space Corporation. Compared to conventional lidar (also called linear lidar, Abdullah, 2016) systems that require hundreds of detected photons to make a range measurement, SPL requires only one detected photon. With such high sensitivity, SPL can divide one light beam into one hundred beamlets, with the surface returns of each beamlet imaged onto one pixel of a 100 pixel detector, and simultaneously make a high-density, multiple-return measurement for a 5m x 5m topographic area from a single outgoing laser pulse. As a result, the increased point density per laser pulse releases the requirement of high pulse repetition rate for linear lidar systems and allows the SPL system to work at much higher altitude and with a wider swath. Such systems have been made available quite recently and are attracting interests from diverse professionals (Abdullah, 2016). In this paper, we will present the results of an initial study on the mapping capabilities and performance of the SPL system by exploring three different sample datasets over forest, urban, and bathymetric areas.

SINGLE PHOTON LIDAR SYSTEMS

Sigma Space has developed three SPL systems so far. The first one is the High Resolution Quantum Lidar System (HRQLS pronounced "Hercules"). Besides HRQLS, two more advanced SPL systems were also recently developed and fielded with both higher operating AGLs (Above Ground Level) and higher measurement rates. The High Altitude Laser (HAL) operates up to 10,668 m (35,000 ft) at 3.2 Megapixels per second, while the upgraded HRQLS-2 operates at a nominal altitude of 3,810 m (12,500 ft) with measurement rates up to six Megapixels per second. The newer models are summarized and compared to HRQLS in Table 1. The nominal AGL is defined as the AGL where the probability of receiving a return per pixel from a 10% reflectance surface (eg., green vegetation) is 95% and roughly 99% from a 15% reflectance surface (eg., soil or dry vegetation). The systems can be operated at substantially higher AGLs than the nominal value (i.e., 5,486 m or 18,000 ft for HRQLS-2 and 10,363 or 34,000 ft for HAL) to achieve wider swaths and greater areal coverage but with reduced detection probabilities per pixel. All are designed to operate at aircraft speeds in excess of 200 knots.

The SPL data used in this study was acquired by HRQLS, whose general parameters are summarized in Table 2. It is designed to operate at an AGL between 1,829 – 4,572 m (6,000 to 15,000 ft). It can operate with either a dual-wedge or single-wedge optical scanner. The dual wedge scanner permits a wide range of scan patterns and swath widths in a single instrument and allows the end user to vary the point density at a given AGL.

DATA USED

The test data was collected in Maryland on Nov. 21, 2014. The location of the areas and the airplane trajectory are displayed in Figure 1. Three datasets of diverse terrain were used in this study: one forest, one urban, and one bathymetric area. The close views of the three dataset areas are shown in Figure 2 with Google Earth images. The Forest dataset was over Idylwild Natural Area in Caroline County. It is part of the Marshyhope Creek watershed and has many ancient sand ridges. A mixture of pines, oaks and heath shrubs can be found in the dry, sandy soils. It is mainly covered by forest except that some bare ground is exposed in the middle-bottom of the image. Several forest

roads are barely visible from the images. The Urban dataset was collected at St. Aubins Heights in the northern part of Easton County. The dataset has an irregular shape. Features in the dataset include residential houses, shopping malls, parking lots, grasses, streets and roads. The Bathymetric dataset was collected at Eastwood Point in Easton County. The water area in the dataset is part of the Tred Avon River, which flows to the North Atlantic Ocean via the Chesapeake Bay.

Table 1. Performance summary of the three SPL systems. The single pass ground coverage is calculated without considering the side-lap which might be up to 30-50% in practice. The mean measurements per square meter assume an aircraft flying at 200 knots and operating in a standard clear atmosphere (15 km visibility) at the nominal AGL. The swath, ground coverage, and mean measurements per square meter vary over the range of scanner cone half angles available to the particular lidar.

SYSTEM	HRQLS	HRQLS-2	HAL
# Beamlets per pulse	100	100	100
Laser fire rate (kHz)	25	60	32
Measurement rate (Mpix/sec)	2.5	6.0	3.2
Nominal AGL (m)	2,286	3,810	7,620
Scanner Cone Half Angle (deg)	Variable: 0 to 20	10,15,20,or 30	9
Swath at nominal AGL (m)	0.5 – 1,664	1,344 - 4,399	2,414
Max. single pass ground coverage at 200 knots (km ² /h)	0.19 to 630	498 to 1,630	894
Mean measurements per sq. m (>15% surface reflectance)	48,596 to 15	43 to 13	13

Table 2. HRQLS parameters and specification.

PARAMETER	SPECIFICATION
# Beamlets per pulse	100
Wavelength	532nm
Laser repetition rate	25kHz
Laser pulse width	700 psec
Laser output power	1.7W
Eye safety	Eye safe by ANSI standards
Multiple return capability	Yes
Pixel recovery time	1.6 nsec
RMS range precision	+/- 5 cm
Scan patterns	Linear, conical, spiral, etc
Scan width	0-40 degrees (selectable)
Operational altitude range (nominal), kft	6.5 – 10 (7.5)*
Swath vs AGL at max scan angle, km	1.4 - 2.2 (1.7)*
Ground coverage vs AGL, single pass at max. scan angle, km ² /hr	534 - 822 (616)*
Mean point density per sq. m, single pass at max scan angle , >15% reflectance surface	17 – 11 (15)*
Size	19 W x 25 D x 33 H inches
Prime power	555 W

*min AGL– max AGL (nominal AGL)

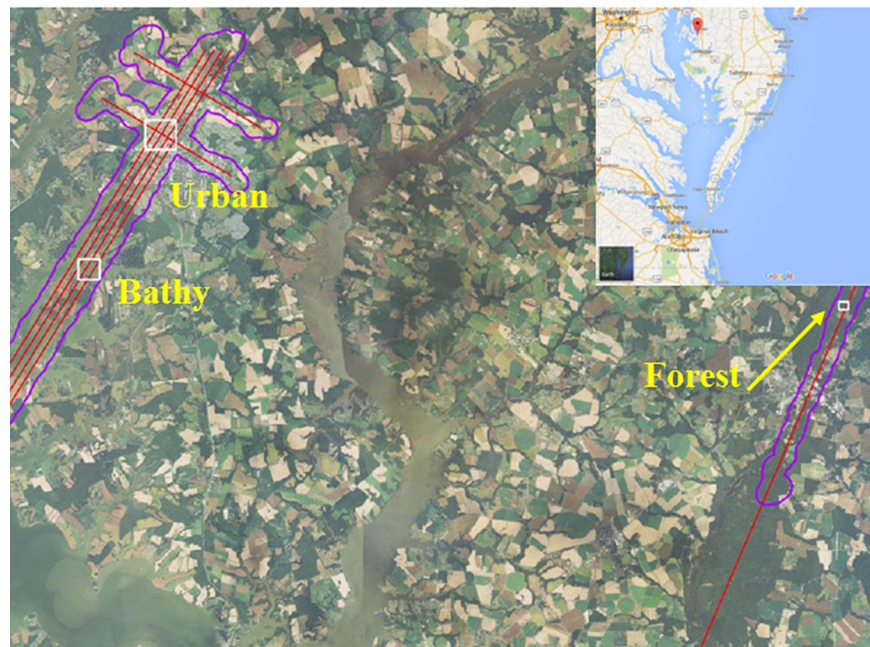


Figure 1. Flight area and the airplane trajectory. An inset map at the upper-right corner shows the location of the study area as an overview. Each red line was flown in two directions. Both directions were included in the Urban and Forest samples; only one direction was included in the Bathy sample.



Figure 2. Images (Google Earth) of the three datasets (from left to right: Forest, Urban and Bathy).

Table 3. Summary of the test datasets collected by the HRQLS system.

DATASET	FOREST	URBAN	BATHY
Location	Idylwild Natural Area	St. Aubins Heights	Eastwood Point
Size (width x height)	403 x 344	1,285 x 1,242	906 x 864
# Passes	2	2	1
# Points	1,403,103	20,385,028	2,954,549
Point density (# per sq. m)	10	18	4
# Ground points after filtering	494,357	12,309,811	789,451
Ground point density (# per sq. m)	3.6	10.1	1.1
Ground spacing (m)	0.52	0.31	0.95

The collection was carried out with a HRQLS system equipped with a single-wedge optical scanner. At a nominal AGL of 2,286 m (7,500 ft) where our data was acquired, the maximum cone half-angle of 10 degrees provides a swath of 806 m. At a flight speed of 165 knots, the coverage rate is 246 km²/h. The point clouds are in las format. The Forest and

Urban areas were covered by two passes, while the Bathy area was mapped in one pass. Properties of the datasets are summarized in Table 3.

FILTERING AND DEM GENERATION

All three datasets were subjected to filtering process to create a digital elevation model (DEM). We extracted the ground points using a filter implemented in the LAStools (<https://rapidlasso.com/>). The number of ground points after filtering is also listed in Table 3. Figure 3 shows the input point clouds (left), the filtered ground points (middle), and the shaded 1 m resolution DEM (right) for the three datasets. As shown in Table 3, the SPL Forest dataset has 494,357 (35.23% of total) ground points at a density of 3.6 points per sq. meter. For the Urban dataset, 12,309,811 (60.39%) points are classified as ground, yielding a ground point density of 10.1 points per sq. meter. For the Bathy dataset, there are 789,451 points left as ground, leading to ground point density 1.1 points per sq. meter.

SPL DEM vs. LINEAR LIDAR DEM (FOREST)

In order to make a comparative analysis, whenever available, we tried to download the point clouds collected by the linear lidar systems from the U.S. Geological Survey (USGS) Earth Explorer website (<http://earthexplorer.usgs.gov/>). We intended to use such point clouds and their derived products as a reference (hereafter called reference DEM) to compare the properties with the SPL data. It turned out that, among the three areas, only the Forest one has such linear lidar point clouds available online. Two files 'MD_Statewide_2003_000798.las' and 'MD_Statewide_2003_000776.las' were found, both of which were collected in June 2003. They were then merged for our study, yielding a total of 119,037 points in the linear lidar dataset with a point density of 0.82 points per sq. meter at a point spacing 1.10 m. Figure 4 shows the point cloud, filtered ground points and the 1 m shaded DEM from the linear lidar over the Forest area. Two dark gaps (labeled by an oval) are visible at the right side of the point clouds, an effect introduced when merging the two files.

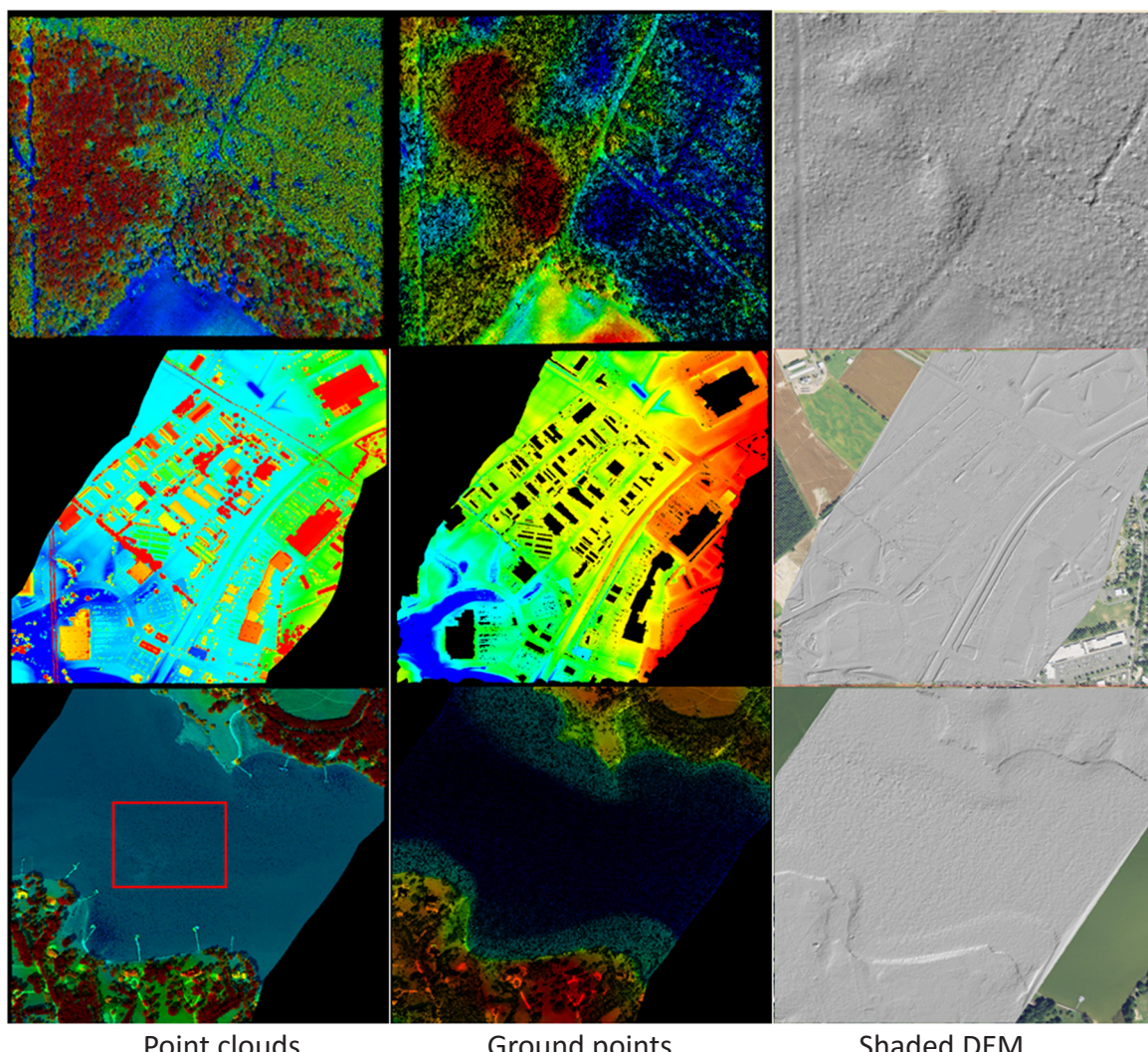


Figure 3. Point clouds (left), ground points (middle) and shaded 1 m DEM (right) from the SPL for the Forest (top), Urban (middle) and Bath (bottom) datasets.

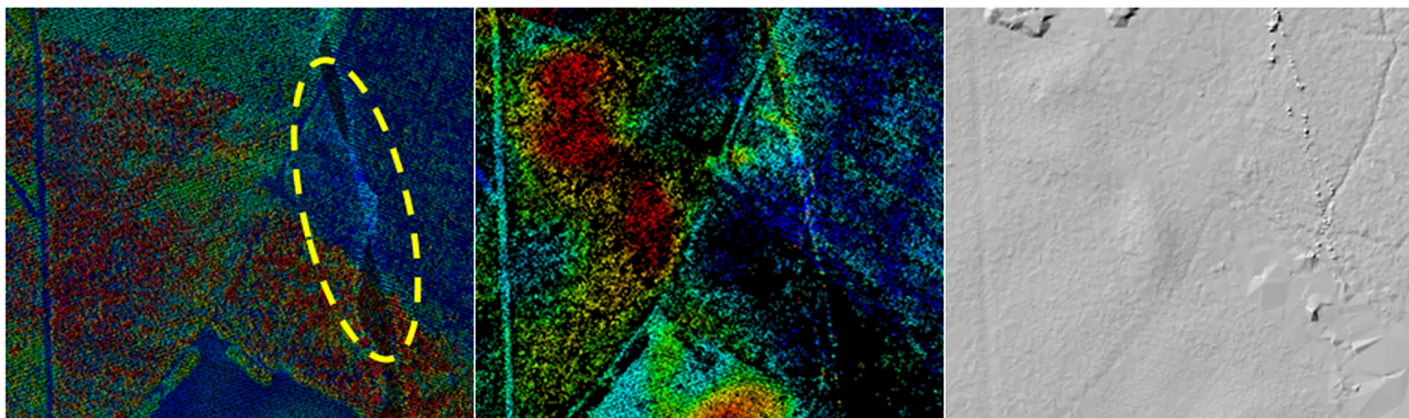


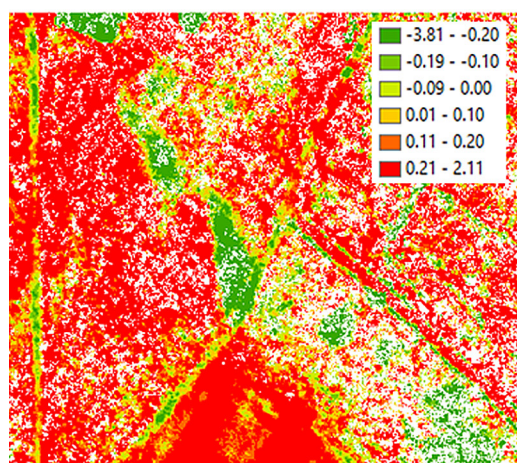
Figure 4. Point cloud (left), filtered ground points (middle) and the 1 m shaded DEM (right) from the linear lidar over the Forest area.

The difference between the two 1 m DEMs as well as its histogram are shown in Figure 5. The majority of the area in Figure 5a appears yellow, suggesting the elevation difference ranges from -0.5 to 0.5 m. The histogram in Figure 5b further reveals the peak difference occurs at a mean of 0.21 m, i.e., the SPL DEM is in general higher by this amount than the reference DEM. Comparing the two shaded reliefs in Figure 4 and Figure 3 for the forest area, we notice that many small fractal, rugged terrain features distributed rather evenly over the study area. With reference to the image shown in Figure 2, it is believed they are small bushes or trees remained in the filtering results. The difference is likely caused by imperfect filtering in forested areas where highly dense multi-stop data is processed. We therefore see a challenging data processing task for new, advanced lidar developments, eg., SPL.

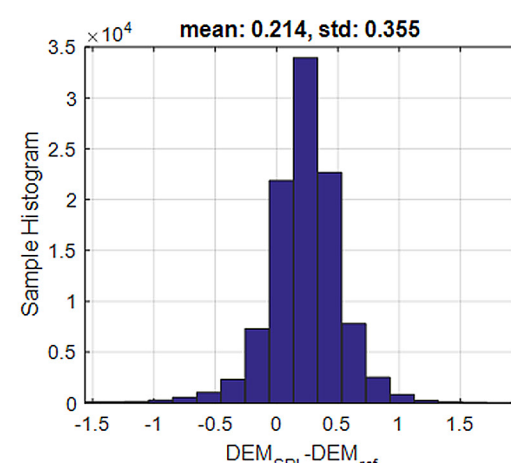
We note that the ground point density of the SPL data after filtering is as high as 3.6 points per sq. meter and the average point spacing reaches 0.52 meters. Such dense points make it theoretically possible to generate DEMs with a resolution higher than 1 meter, except areas under dense trees. To

explore the potential of the SPL data, Figure 6 provides the DEMs with 0.5 m, 0.25 m and 0.1 m resolutions. We can see that the DEM with higher resolution presents less noise than the lower ones. For example, the height difference along the forest roads becomes less obvious as the resolution increases. This can also be observed if we compare the SPL DEMs in Figure 6 with the 1 m linear lidar DEM in Figure 3, where the most significant differences can be found along the roads or trails under canopy.

Finally, we would like to look into the distribution of the point density. After filtering, the linear lidar dataset has 37,512 (31.51%) ground points left, corresponding to a point density 0.26 points per sq. meter at a ground spacing 1.96 meters. When compared to the SPL Forest dataset in Figure 3 and Table 3, the raw SPL data is 12.2 times (10/0.82) denser as the linear lidar data, but its ground point density after filtering is as 13.8 times (3.6/0.26) higher. However, it should be noted that the distribution of remaining ground points is not even, as depicted by the point density in Figure 7. For comparative purpose, the figure also depicts the distribution



(a)



(b)

Figure 5. Difference of the SPL and linear lidar DEM (in meters) and its histogram of the Forest dataset.

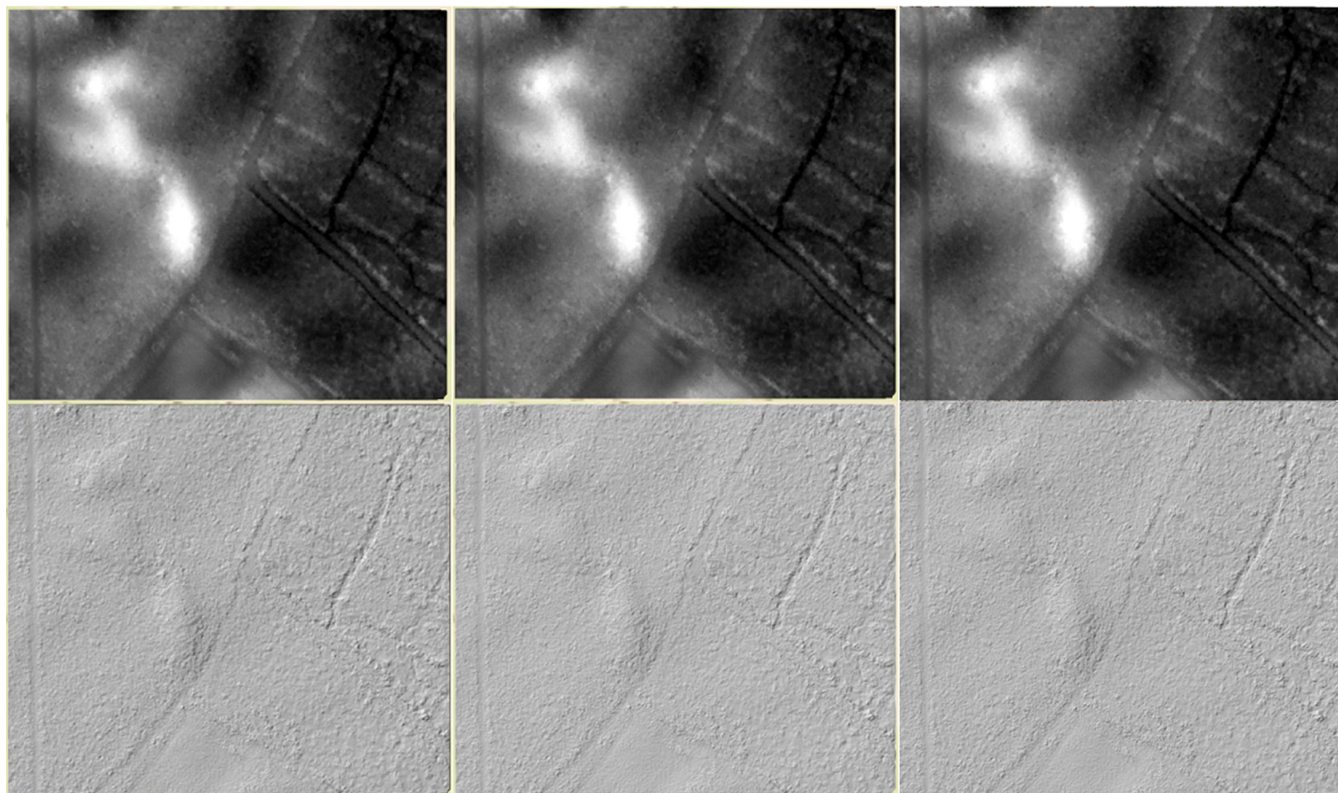


Figure 6. Higher resolution SPL DEM (top) and shaded DEM (bottom) at a resolution of 0.5 m (left), 0.25 m (middle) and 0.1 m (right) over the Forest area.

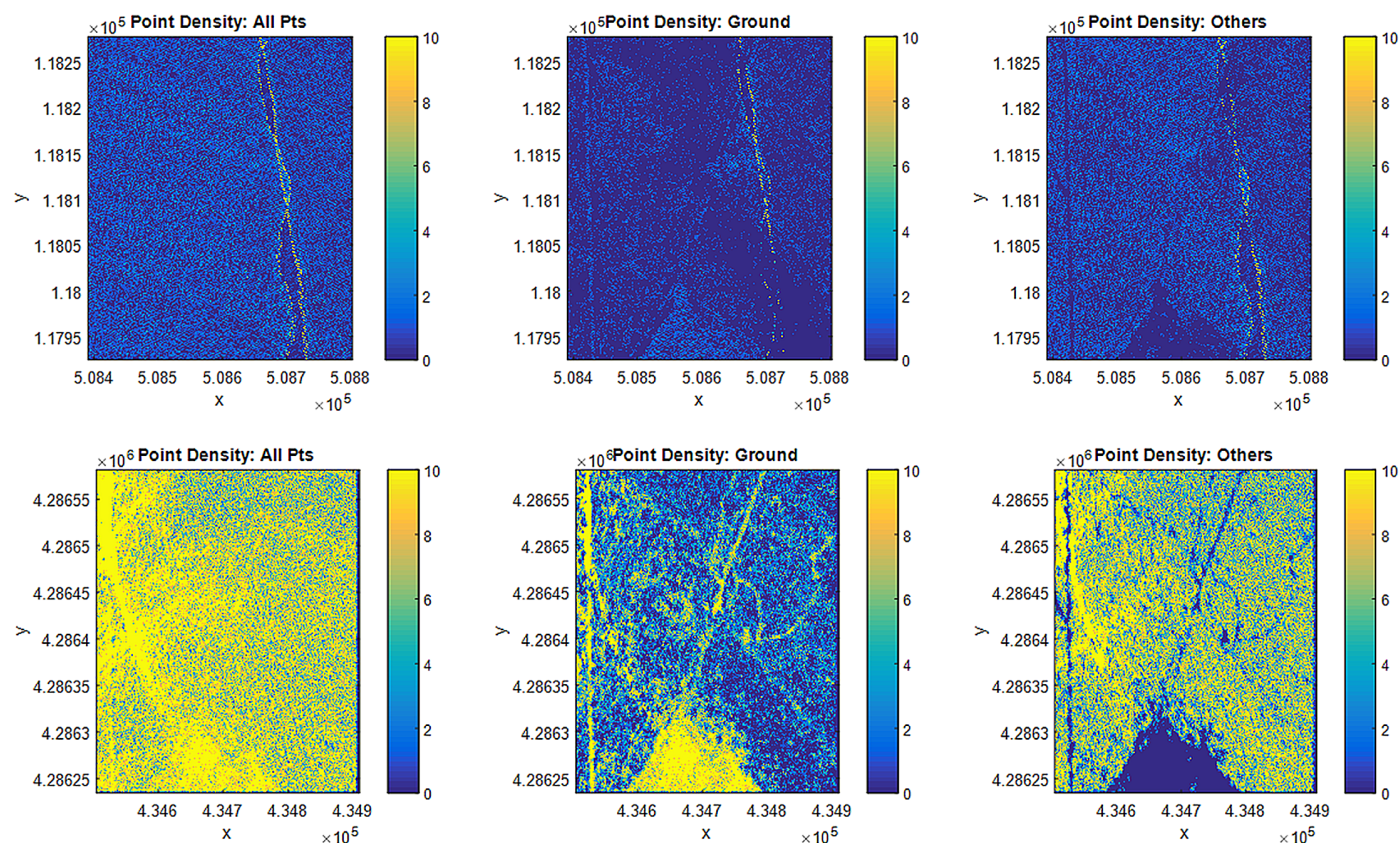


Figure 7. Distribution of point density of the linear lidar (top) and the SPL (bottom). The three columns are the density (#points/sq. meter) of all points (left), ground points (middle) and non-ground points (right).

of point density of the linear lidar data, which was collected in leaf-on season (June). In fact, many SPL ground points are located in the lower middle triangle region where little forest exists. The SPL point density for the majority of the ground is 1.0-2.0 points per sq. meter, i.e. the vast majority of the SPL raw points are from forest canopy. This ground point density is still as 3.8 - 7.7 times higher than the linear lidar density. However, since the SPL data was collected in leaf-off season (November), we could not conclude if the same or equivalent point density would still be expected when operated in leaf-on season. The 'penetration' capability of SPL remains to be further investigated.

UNCERTAINTY OF SPL MEASUREMENTS

We intended to study the performance of SPL by looking into its interaction with specific ground features. To this end, we selected three roofs from the Urban dataset. In addition, a small pond in the south part of the same dataset was also selected, which can be assumed to be perfectly flat. Figure 2 (middle) marks the locations of the three roofs and the pond. The point clouds of the three roofs and their elevation histograms are shown in Figure 8, which shows that none of the roofs are perfectly flat. Roof 1 has several small high-rise attachments,

while Roof 2 and 3 are slightly sloped. The height standard deviations are 0.13 m, 0.17 m and 0.28 m, respectively for the three roofs. We cannot imply the vertical uncertainty of the SPL sensor by using the three roof samples, but it is safe to say that it is able to detect height differences at a magnitude of at least 0.2 m.

As for the pond, Figure 9 shows a section of its street view, the SPL points, and the corresponding height histogram. A peak pulse in the height histogram is found at 4.71 m, which should be the height of the pond with respect to the vertical datum. The standard deviation 0.09 m of the histogram then likely comes from SPL's noise or sensitivity and suggests the intrinsic uncertainty of the SPL measurements.

To further investigate and verify the sensitivity of SPL, we repeated our work on water pond for the river water in the Bathy dataset. In Figure 10, we selected a sample of $364 \times 340 \text{ m}^2$ from the water area marked by the red box in Figure 3. There are 291,547 points in total. Some of them are on the riverbed, and the others are on the water surface. We extracted the water surface points by vertically reversing the data and running ground filtering. It returned 190,253 'ground' points that are the water surface, yielding a point density of 1.5 points per sq. meter and ground spacing 0.82 m. The height histograms

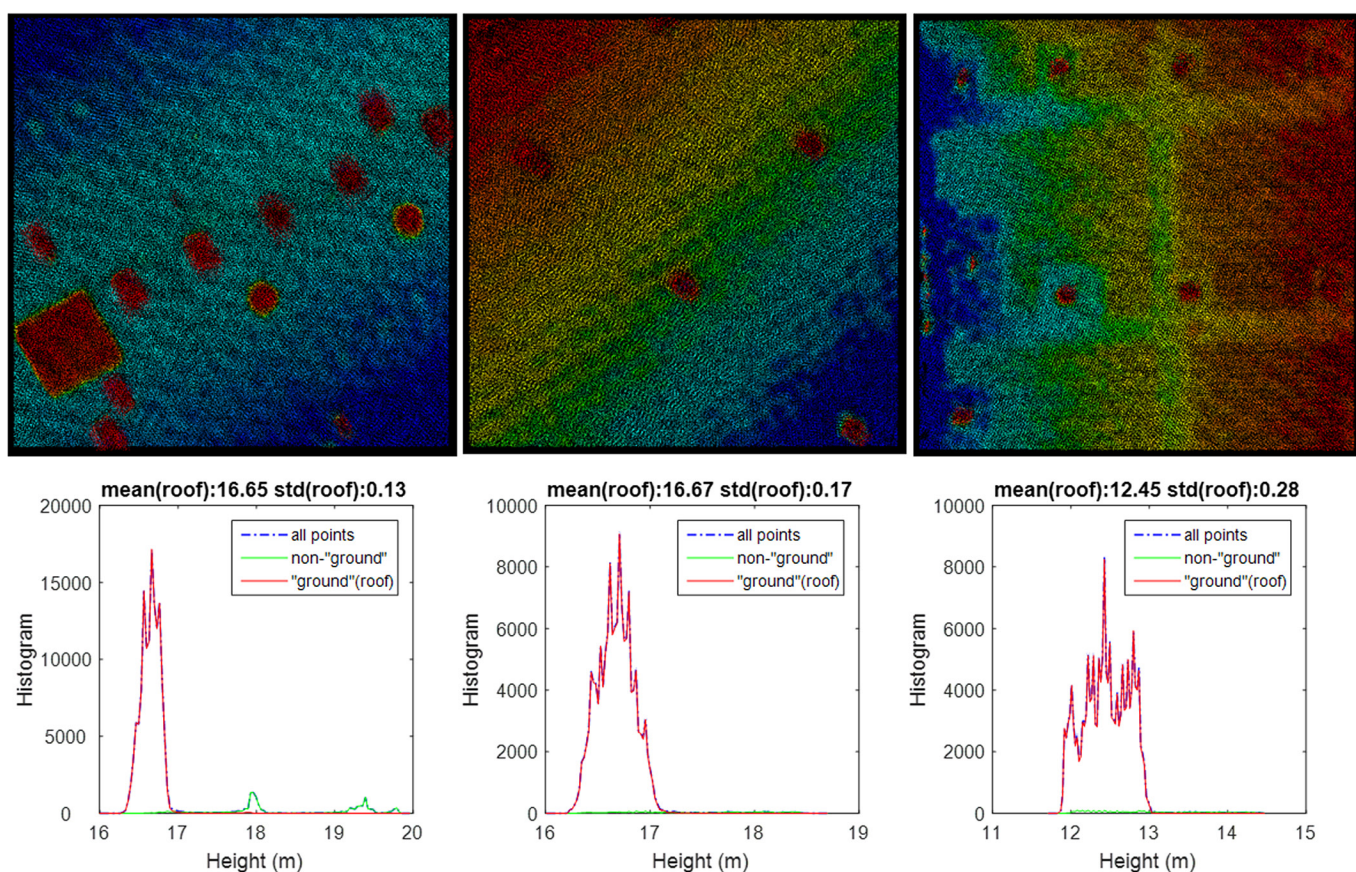


Figure 8. The SPL point clouds (top) and their height histograms (bottom) for the three roofs.

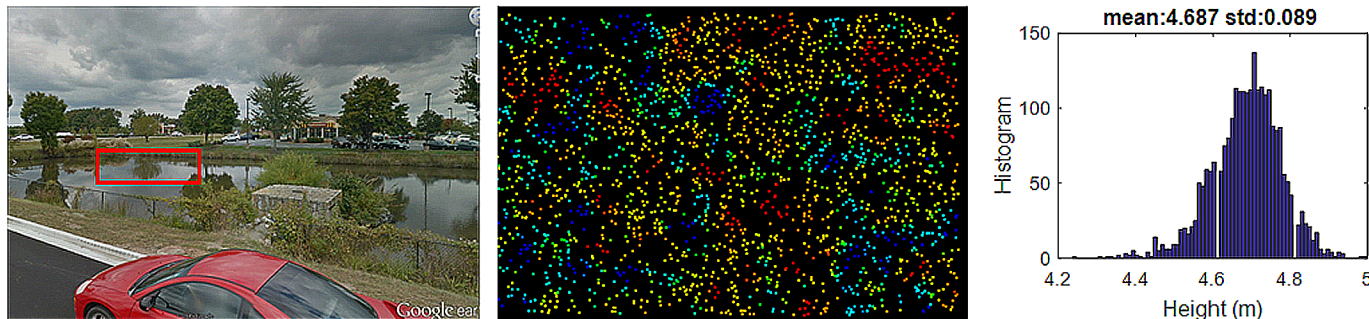


Figure 9. Google Street View (left), SPL points (middle) and height histogram (right) of the selected water pond area (the small red box).

for all points, water surface points and non-water points are shown in Figure 10a. We then generated a 1 m DEM (Figure 10b) from the water surface points. Several noisy spots are visible in the north, since they are shallow waterbed and close to the shore, leading to an imperfect filtering. The mean height of the filtered water surface points is 0.13 m above the vertical datum and the standard deviation is 0.12 m. If we compare this with our previous observation on the pond, we are able to conclude that the height sensitivity of SPL is in the range of 0.09 – 0.12 m. It should be noted that the pond water should be quite still, while the river water surface in the Bathy dataset connects to the Chesapeake Bay, with possible minor water waves; hence a slightly larger height variation of 0.12 m is observed.

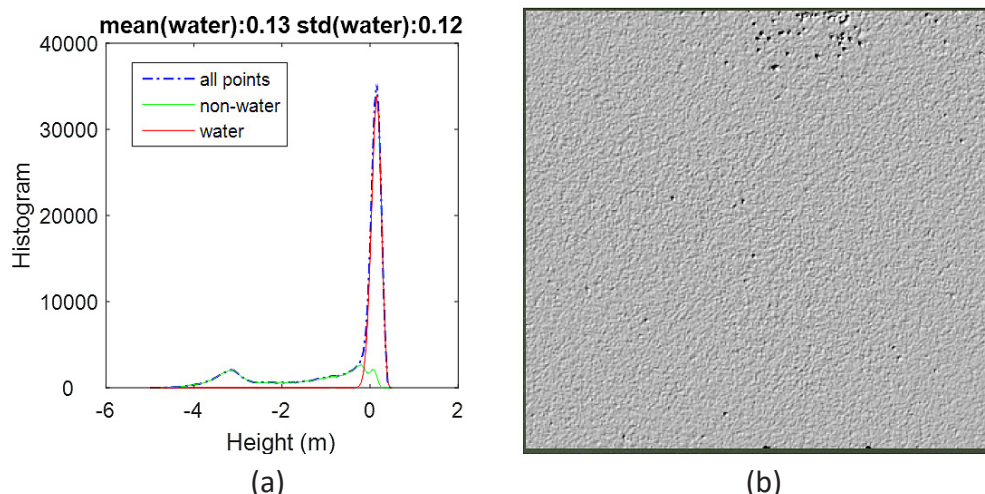


Figure 10. The height distribution of the SPL points (a) and the 1 m water surface shaded DEM (b) for the selected river water area in the Bathy dataset.

CONCLUSION

Single photon laser has opened an exciting opportunity for lidar topographic mapping. It can simultaneously transmit hundreds of beams and record single photon returns. This allows data collection to be carried out in a much higher altitude and a much higher rate than the conventional linear lidar. The SPL datasets used in this paper were collected at an altitude of 2,286 m (7,500 ft). The SPL was able to generate a spatial resolution over 10 times denser than what

a conventional lidar can possibly achieve even at a much lower altitude (a few hundred meters), thus causing a smaller swath and lower productivity for the linear systems.

The high density of single photon lidar poses a new challenge to the ground filtering process for digital elevation model generation. It is shown majority of the returns in forest are from tree canopy, while only a small portion of the returns are actually from the ground. Taking the forest dataset as an example, the filtered ground returns under canopy are only as 3 – 7 times more as the linear lidar. As a result, we may not optimistically expect that terrain generation will benefit from the new systems as much as tree canopy inventory would, though this statement depends on the canopy density

in general. Because of higher density over canopy area, local canopy tends to be treated as flat and therefore wrongly classified as ground, leading to visible artifacts in the resultant digital elevation model. This study has demonstrated a critical need to revisit existing popular filtering methods and explore new ones to accommodate recent developments in lidar systems. Similarly, the ‘penetration’ capability of such new systems in leaf-on seasons is worthwhile of further investigation.

The intrinsic uncertainty of elevation measurements for the SPL system is another factor that we looked into. This

was an independent effort in addition to using laboratory calibration or ground control. Instead, we intended to use natural features that have known geometric properties. The water pond and the river water examples demonstrated that the SPL system has an intrinsic elevation uncertainty of 0.09 – 0.12 m. Besides, this was supported by the fact that small, low roof objects at a height of 0.20 m could be easily detected.

Finally, although the capability of acquiring highly dense

point cloud over a large area in an unparalleled speed is of a reality, the data processing and applications are still at the infant stage. One needs to do more to explore the potentials of such new technology and make further efforts, especially in terms of data processing and product delivery, to make this technology beneficial to the mapping community.

REFERENCES

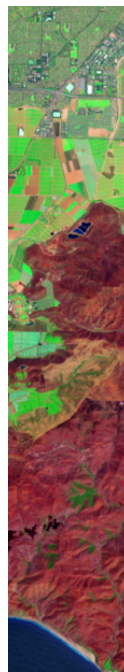
- Abdullah, Q. A., 2016. A Star is Born: The State of New Lidar Technologies. *Photogrammetric Engineering and Remote Sensing*, Vol. 82, No. 5, pp. 307-312
- Degnan, J., C. Field, T. Barrett, B. Tesfaye, S. Disque, R. Machan, E. Leventhal, Y.H. Zheng, C. Ventura, D. Caplan, and J. Marcos Sirota, 2015. Applications of Lasers for Sensing and Free Space Communications, Proceedings *Imaging and Applied Optics 2015*, DOI: 10.1364/LSC.2015.LM3D.4

AUTHORS

Qinghua Li is with the Lyles School of Civil Engineering, Purdue University, West Lafayette, IN 47907, USA

John Degnan and **Terence Barrett** are with Sigma Space Corporation, 4600 Forbes Blvd., Lanham, MD 20706, USA

Jie Shan, corresponding author, is with the Lyles School of Civil Engineering, Purdue University, West Lafayette, IN 47907, USA, jshan@purdue.edu.



GeoBytes!

ASPRS GIS DIVISION — FREE ONLINE SEMINARS

The ASPRS GIS Division, in cooperation with CaGIS and GLIS, is sponsoring free online live seminars throughout the year.

Attention those seeking ASPRS Certification: ASPRS Online Seminars are a great way to gain Professional Development Hours!

<http://www.asprs.org/GISD-Division/Online-Seminars.html>

STAND OUT FROM THE REST EARN ASPRS CERTIFICATION

ASPRS congratulates these recently Certified and Re-certified individuals:

RECERTIFIED PHOTOGRAHMETRISTS

Timothy Cooke, Certification #R1013
Effective May 16, 2016, expires May 16, 2021

Philip Gershkovich, Certification #R1500
Effective July 30, 2016, expires July 30, 2021

Mark A. Hammond, Certification #R966

Effective September 19, 2015, expires September 19, 2020

David M. Hart, Certification #R1295

Effective March 27, 2016, expires March 27, 2021

Maria Alicia C. Ramos, Certification #R1277

Effective November 28, 2015, expires November 28, 2020

RECERTIFIED PHOTOGRAMMETRIC TECHNOLOGIST

Nathan Kempf, Certification # R1440PT
Effective March 10, 2016, expires March 10, 2019

RECERTIFIED MAPPING SCIENTIST REMOTE SENSING

Eric Zehnbauer, Certification # R232RS
Effective September 20, 2015, expires September 20, 2020

ASPRS Certification validates your professional practice and experience. It differentiates you from others in the profession.

For more information on the ASPRS Certification program: contact certification@asprs.org, visit <http://www.asprs.org/membership/certification>

 THE
**IMAGING & GEOSPATIAL
INFORMATION SOCIETY**

